Design and characterization of semiconductor-doped silica film saturable absorbers

Rohit P. Prasankumar, Ingmar Hartl, Juliet T. Gopinath, Erich P. Ippen, and James G. Fujimoto

Department of Electrical Engineering and Computer Science and Research Laboratory of Electronics, Massachusetts Institute of Technology, Cambridge, Massachusetts 02139

Paul Mak and Michael F. Ruane

Photonics Center, Department of Electrical and Computer Engineering, Boston University, Boston, Massachusetts 02215

Received August 29, 2003; revised manuscript received November 18, 2003; accepted December 3, 2003

Nonepitaxially grown, rf sputtered semiconductor-doped silica film saturable absorbers have recently been developed as a versatile, easy to fabricate, cost-effective alternative to epitaxially grown semiconductor saturable absorbers. Characterization of their linear and nonlinear optical properties reveals trends that permit the development of guidelines for optimizing these devices for a particular laser system. Operation near the onset of absorption, the use of films with large nanocrystallites, and high rapid thermal annealing temperatures result in saturation fluences as low as 640 $\mu J/cm^2$ at 1.54 μm. These materials can be used to start Kerr-lens mode locking in a wide range of solid-state lasers. © 2004 Optical Society of America

OCIS codes: 320.7130, 160.4330, 320.032, 320.7090.

1. INTRODUCTION

Ultrafast laser technology has rapidly matured in recent years, resulting in widespread research applications of ultrafast solid-state laser systems. Although Kerr-lens mode locking (KLM) has been applied to a wide range of solid-state lasers,[1,2] self starting mode locking is difficult to achieve.[3] Epitaxially grown semiconductor saturable absorbers are a well-established technology for direct mode locking as well as for starting KLM in solid-state lasers. These devices, known as semiconductor saturable-absorber mirrors or saturable Bragg reflectors, typically consist of semiconductor quantum wells grown in a semiconductor mirror structure by molecular beam epitaxy.[4–7] Epitaxially grown semiconductor saturable-absorber mirrors and saturable Bragg reflectors have the advantage of low saturation fluences in the 10–100-$\mu J/cm^2$ range.[5] Semiconductor saturable-absorber mirrors and saturable Bragg reflectors have been successfully used in mode-locking solid-state lasers, helping to start and support few-cycle pulses in a Ti:sapphire laser.[8] However, they suffer some disadvantages, such as lattice matching constraints that limit the choice of semiconductor materials as well as the requirement of complicated, expensive fabrication equipment. In addition, the bandwidth of these devices is typically limited, and postprocessing is often required for fabrication of broadband devices,[9] although more recently epitaxially grown devices were fabricated that overcame some of these restrictions.[10]

Nonepitaxially grown saturable absorbers based on semiconductor nanocrystallites doped into glass structures are a low-cost, simple, and versatile technology for mode-locking applications. Semiconductor-doped glass structures based on colored glass filters were developed and used to self-start mode locking in solid-state lasers, generating pulses as short as 52 fs.[11–13] More recently, nonepitaxially grown, rf sputtered saturable-absorber devices have been developed and applied to self-starting KLM in Ti:sapphire and Cr:forsterite lasers.[14,15] The saturable-absorber devices consist of InAs nanocrystallites doped into SiO_2 films and deposited upon sapphire substrates by magnetron and nonmagnetron rf sputtering systems. Rf sputtering is an inexpensive, simple device-fabrication technique that offers flexibility in the choice of semiconductor dopant and substrate materials.[16–19] This technique allows the deposition of semiconductor-doped silica films onto almost any substrate with no lattice-matching constraints. Any of a variety of semiconductors can be chosen as the dopant. Changing the semiconductor dopant and nanocrystallite size permits control of the optical absorption edge. The linear absorption coefficient is directly proportional to the doping density, and one can easily scale the total absorption by changing the film thickness. The broad nanocrystallite size distribution leads to a broad bandwidth of operation. These semiconductor-doped silica films can be deposited with much higher doping densities than bulk semiconductor-doped glasses, facilitating simple deposition in a thin layer upon a variety of substrates including mirror structures. Finally, rapid thermal annealing (RTA) in nitrogen at 500–750 °C was found to be an effective method to control the absorption saturation dynamics of the saturable absorbers.[20] Studies of semiconductor-doped silica films as saturable absorbers in KLM femtosecond Ti:sapphire lasers were performed, and self-starting 25-fs pulses with a bandwidth of 53 nm and a tuning range of 80 nm were obtained.[14] The primary drawback of these saturable-absorber films was their high saturation fluence, measured to be 25 mJ/cm^2.

0740-3224/2004/040851-07$15.00 © 2004 Optical Society of America

A low saturation fluence is desirable for avoiding Q-switched mode-locking instabilities, facilitating saturable-absorber mode locking without KLM and exploiting the full modulation depth of the saturable absorber.[21] Epitaxially grown saturable absorbers typically have low saturation fluences[5] and therefore do not suffer from these limitations.

The goal of the present study is to comprehensively characterize the linear and nonlinear optical properties of semiconductor-doped silica film saturable absorbers to develop guidelines for designing these devices with optimized saturation fluence for a given solid-state laser system. The influence of fabrication parameters on the optical properties of the saturable-absorber devices is measured by use of linear transmission and pump–probe experiments to determine the most important factors that influence device performance. The design guidelines developed from these experiments have permitted the design and fabrication of semiconductor-doped silica films for mode locking a Cr:forsterite laser with nearly an order-of-magnitude reduction in saturation fluence compared with the device previously used to mode lock Ti:sapphire.[15]

2. METHODS OF FILM DEPOSITION

The semiconductor-doped silica films used in these experiments were deposited by a Denton Discovery 18-magnetron rf sputtering system. The rf frequency was 13.56 MHz, and the rf power was 100 W. All films were deposited upon sapphire substrates, with the substrate temperature approximately 25 °C during each sputtering run. The films were annealed in nitrogen after deposition. We varied parameters including the choice of semiconductor and glass materials, pump–probe wavelengths relative to the onset of absorption, annealing time and temperature, and ratio of semiconductor to glass to determine their effect on the saturation fluence.

The effect of varying the ratio of InAs to SiO_2 on the size of the InAs nanocrystallites in the silica films was tested. It has been shown[16,18,19] that varying the ratio of semiconductor to glass on the target can be used to control the nanocrystallite size in the sputtered film. Larger semiconductor-to-glass ratios result in larger nanocrystallite sizes in the deposited film, shifting the optical absorption edge to longer wavelengths. Films with ratios of 3% InAs/97% SiO_2, 10% InAs/90% SiO_2, and 40% InAs/60% SiO_2 were deposited upon sapphire substrates by rf sputtering and annealed in nitrogen at 600 °C. Linear transmission measurements (Fig. 1) performed with a Cary 5E spectrophotometer revealed a shift of the onset of absorption to longer wavelengths for higher InAs/SiO_2 ratios, as expected. The onset of absorption is at ~950 nm for the 3% InAs/97% SiO_2 film, ~1200 nm for the 10% InAs/90% SiO_2 film, and ~1700 nm for the 40% InAs/60% SiO_2 film. The size distribution of the nanocrystallites also appears to increase with InAs/SiO_2 ratio, as one can see from the more gradual slope in the transmission curves. Varying the semiconductor-to-glass ratio is a simple and effective way to control the nanocrystallite size in the sputtered films, enabling films to be fabricated for operation at several laser wavelengths over a broad range with only a single semiconductor material.

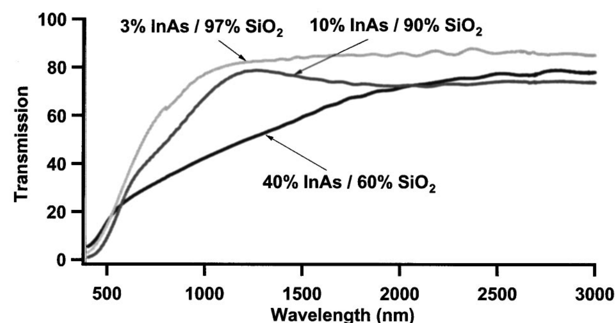

Fig. 1. Linear transmission measurements for films with different InAs/SiO_2 ratios, revealing a shift of the absorption edge toward longer wavelengths with higher ratios of semiconductor to glass.

3. WAVELENGTH-TUNABLE PUMP–PROBE SYSTEM

Nonlinear optical pump–probe measurements were performed with a femtosecond $Ti:Al_2O_3$-laser-based pump–probe system with 17-fs time resolution and independent pump and probe wavelength tunability over a range of 700–1000 nm. A schematic of this system is shown in Fig. 2. The broad wavelength coverage and high resolution were made possible by use of a broadband $Ti:Al_2O_3$ laser operating at a 100-MHz repetition rate with pulse durations as low as 5.5 fs, bandwidths exceeding 300 nm, and average powers of 100–120 mW.[22] A broadband beam splitter (BS) splits the output of the laser into pump and probe beams. The two beams are directed into individual prism compressors, each consisting of two fused-silica prisms separated by 135 cm.[23] In each prism compressor the pump (probe) beam is spectrally dispersed on a silver mirror after the second prism. Variable slits are positioned near the silver mirror to permit the desired pump and probe wavelengths to be selected. The pump (probe) beam is retroreflected through the prisms in each arm and sent to a standard noncollinear pump–probe setup. We cross polarize the pump and the probe to minimize pump scattering by inserting a broadband half-wave plate in the probe arm. The two beams are focused to a spot size of 20 μm onto the sample with a 5-cm radius of curvature (ROC) parabolic mirror to prevent dispersion from focusing lenses. An aperture and a polarizer are used to block the scattered pump light, and the probe signal is focused by a 5-cm focal-length lens onto the detector.

The time resolution of this system was measured by intensity autocorrelation with a 100-μm-thick β-barium borate crystal. The minimum width of the autocorrelation was 17 fs for the full laser bandwidth in both pump and probe arms, setting the minimum experimental time resolution. The increased pulse duration was due to broadening of the initial sub-10 fs pulses caused by residual uncompensated higher-order dispersion in the prism compressors. No significant change in the time resolution was observed when the laser bandwidth was spectrally filtered in the prism compressors because the mini-

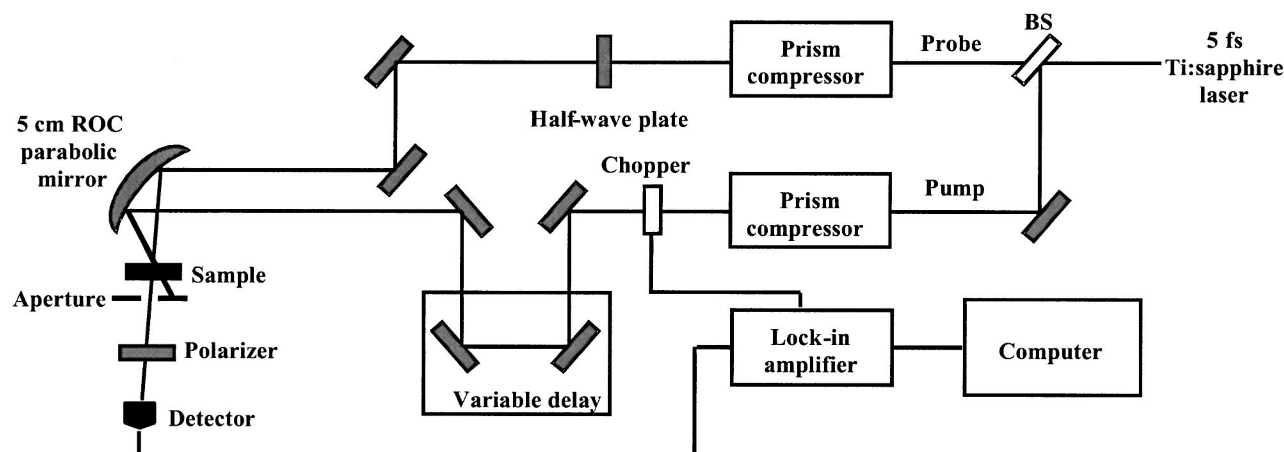

Fig. 2. Schematic of the experimental setup of the noncollinear Ti:sapphire-based pump–probe system with independently tunable pump and probe wavelengths from 700 to 1000 nm.

mum laser bandwidth used in these experiments was 100 nm in each arm, enough to support a 17-fs time resolution.

Pump–probe measurements permit measurement of saturation fluence. For small changes in absorption, saturation fluence Γ_{sat} of a sample can be calculated from the magnitude of the pump–probe signal ($-\Delta\alpha/\alpha$, the change in the absorption coefficient on ultrashort-pulse excitation normalized to the low-intensity absorption coefficient) if the incident fluence Γ is known, from the relation $\Gamma/\Gamma_{\mathrm{sat}} \approx -\Delta\alpha/\alpha$. However, this method of measuring the saturation fluence suffers from some measurement uncertainty because of difficulty in accurately measuring the spot size at the focus.

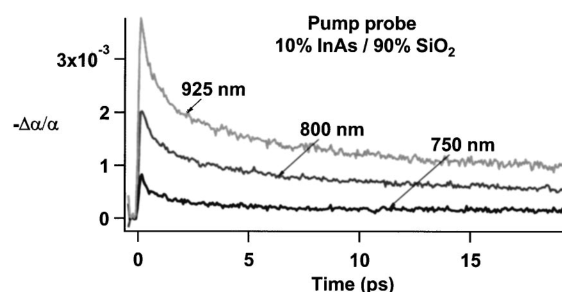

Fig. 3. Degenerate pump–probe measurements of a 10% InAs/90% SiO_2 film as a function of wavelength. The pump–probe measurements show a decrease in saturation fluence with excitation wavelengths closer to the onset of absorption. The measured saturation fluences were 9.3 mJ/cm^2 at 925 nm, 17.5 mJ/cm^2 at 800 nm, and 42.5 mJ/cm^2 at 750 nm.

4. MEASUREMENTS OF ABSORPTION SATURATION DYNAMICS

In initial experiments we examined the saturation fluence near the onset of absorption in a 10% InAs/90% SiO_2 film in a degenerate pump–probe measurement at wavelengths of 750, 800, and 925 nm, using the tunable femtosecond Ti:Al_2O_3 pump probe system (Fig. 3). The measurement at 800 nm used the full laser bandwidth of 250 nm, whereas the measurements at 750 and 925 nm each had a bandwidth of 100 nm centered about the center wavelength. The pump and probe powers at all center wavelengths were 40 and 0.2 mW, respectively. The dynamics at all wavelengths showed a fast decrease in the absorption saturation caused by carrier scattering out of the excited state, followed by a slower recovery time caused by thermalization of carriers and band filling. The measured saturation fluences were 9.3 mJ/cm^2 at 925 nm, 17.5 mJ/cm^2 at 800 nm, and 42.5 mJ/cm^2 at 750 nm. The saturation fluence of this film decreased with increasing wavelength, demonstrating that operation close to the onset of absorption is desirable to minimize the saturation fluence.

These results suggested that a similar wavelength dependence would be observed on examination of the 40% InAs/60% SiO_2 films near their onset of absorption. We used a pump–probe system operating at 1.5 μm to measure the dynamics of the 40% InAs/60% SiO_2 films near their absorption edge of ~1.7 μm. The pump–probe system was based on a Ti:sapphire-pumped optical parametric oscillator (Spectra-Physics Opal) generating 150-fs transform-limited pulses at an 82-MHz repetition rate, with wavelengths tunable from 1.4 to 1.6 μm. The pump and probe powers were 124 and 8 mW respectively, focused to a 20-μm spot on the sample. The results of pump–probe measurements of a 40% InAs/60% SiO_2 film are depicted in Fig. 4.

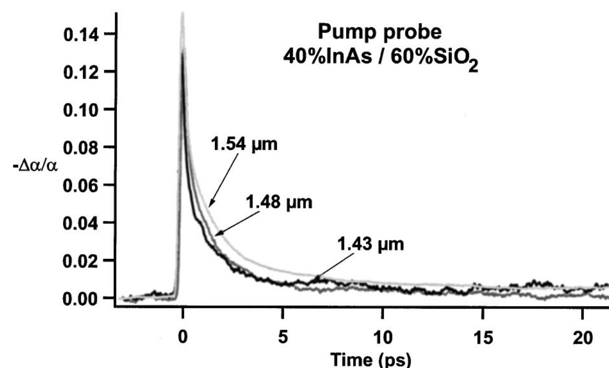

Fig. 4. Tunable degenerate pump–probe measurements on a 40% InAs/60% SiO_2 film at three wavelengths. A saturation fluence of 640 μJ/cm^2 at 1.54 μm was measured.

Several observations can be made from this measurement. As anticipated, the saturation fluence decreased with wavelength over the measured range (1.43–1.54 μm), although the decrease is not so drastic for this sample as for the 10% InAs/90% SiO_2 film shown in Fig. 3. This result is expected because the transmission curve of the 40% InAs/60% SiO_2 film is much smoother than that of the 10% InAs/90% SiO_2 film. It is worth mentioning that pump–probe measurements of 3% InAs/97% SiO_2 films at wavelengths of 750, 800, and 900 nm (not shown) revealed a decrease of the saturation fluence with wavelength as well. Therefore the saturation fluence consistently decreases as the pump–probe wavelength is tuned closer to the onset of absorption.

Perhaps the most important observation from Fig. 4 is the magnitude of the signal, as the peak $-\Delta\alpha/\alpha$ signal is nearly 2 orders of magnitude larger for 40% InAs/60% SiO_2 films at 1540 nm (Fig. 4) than for 10% InAs/90% SiO_2 films at 800 nm (Fig. 3). The saturation fluence for the 40% InAs/60% SiO_2 film was calculated from the pump pulse energy and spot size to be 640 $\mu J/cm^2$ at 1.54 μm. A significantly higher saturation fluence of 72 mJ/cm^2 was subsequently measured on this film at 800 nm. We can understand this higher fluence by noting that the 1.54-μm pump–probe wavelength in Fig. 4 is much closer to the $\sim$1.7-μm onset of absorption and that therefore the wavelength dependence of the saturation fluence has a strong effect. It is also important to note that the 640-$\mu J/cm^2$ saturation fluence of the 40% InAs/60% SiO_2 films at 1.54 μm is more than an order of magnitude lower than the 9.3 mJ/cm^2 saturation fluence of the 10% InAs/90% SiO_2 films at 925 nm, even though both films were measured near their respective onsets of absorption. This result suggests that the increase in nanocrystallite size from the 40% InAs/60% SiO_2 films to the 10% InAs/90% SiO_2 films was responsible for the decrease in saturation fluence.

To further test this hypothesis, we performed pump–probe measurements on annealed 40% InAs/60% SiO_2 films at 1260 nm, using a pump–probe system based on a Cr:forsterite laser for comparison with the previous measurements at 800 nm of the annealed 10% InAs/90% SiO_2 films that were shown in Fig. 3. We chose the wavelengths to be $\sim$400 nm above the onset of absorption in each sample to obtain wavelength-dependent measurements that were analogous to those in the previous experiments. The pump–probe system was a standard noncollinear pump–probe setup, without any prism compressors for spectral filtering. The laser source was based on a Cr:forsterite laser producing pulses as short as 14 fs with a 250-nm bandwidth and average powers of 80 mW at a 100-MHz repetition rate.[24] We reconfigured the laser to operate with average powers of 120 mW and pulse durations of 35 fs for these experiments by increasing the output coupling to 3%. The pump power was 70 mW and the probe power was 0.7 mW, and the beams were focused to a 20-μm spot on the sample. Figure 5 shows pump–probe measurements on the 40% InAs/60% SiO_2 and 10% InAs/90% SiO_2 films. These results show that the magnitude of the pump–probe signal is significantly larger for the 40% InAs/60% SiO_2 film than for the 10% InAs/90% SiO_2 film. The 10% InAs/90% SiO_2 film had a saturation fluence of 17.5 mJ/cm^2 as previously measured. A saturation fluence of 4.05 mJ/cm^2 at 1260 nm was measured for the 40% InAs/60% SiO_2 film. This value was significantly lower than the 25 mJ/cm^2 of the films previously used for mode locking Ti:sapphire.[14] These data demonstrate that saturation fluence, measured at comparable wavelengths above the onset of absorption, decreases with increasing nanocrystallite size.

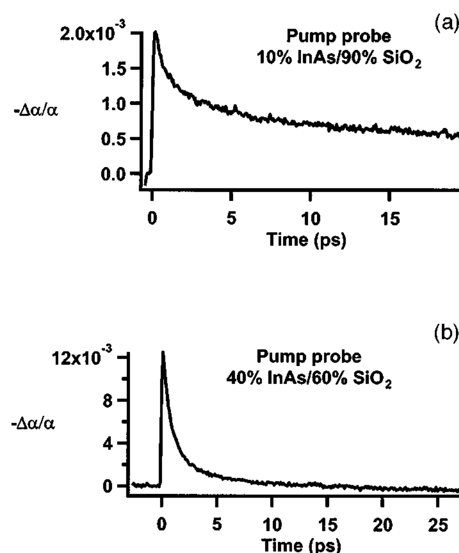

Fig. 5. (a) Degenerate pump–probe measurement at 800 nm of a 10% InAs/90% SiO_2 film. The saturation fluence is 17.5 mJ/cm^2, as described in the text. (b) Degenerate pump–probe measurement at 1260 nm on a 40% InAs/60% SiO_2 film. The saturation fluence was 4.05 mJ/cm^2.

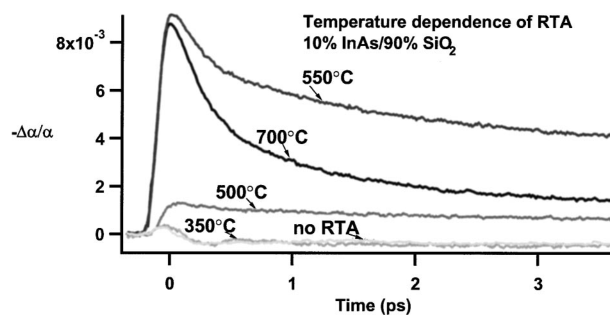

Fig. 6. Degenerate pump–probe measurement of a 10% InAs/90% SiO_2 film at 800 nm. Measurements were made of films prepared with several rapid thermal annealing temperatures. Discrete changes in the absorption saturation dynamics as a function of film annealing temperature are shown.

We varied the annealing temperature of 10% InAs/90% SiO_2 films to determine the effect of RTA on the nonlinear absorption saturation dynamics. Annealing is expected to modify the surface properties of the nanocrystallites; nanocrystallites with better surface properties are anticipated to have lower saturation fluence. Figure 6 depicts the changes in the measured pump–probe signal at 800 nm as a function of annealing temperature for 10% InAs/90% SiO_2 films annealed for 60 s in nitrogen. Distinctive changes in the absorption saturation dynamics were observed as the annealing temperature was varied from 350 to 700 °C. For an unannealed

sample as well as for a sample annealed at 350 °C, a negative pump–probe signal was measured, most likely as a result of excited-state absorption. In the range 400–500 °C the absorption saturation was positive but small. At temperatures of 550 °C and above, the absorption saturation was large; samples annealed at these higher temperatures self-started KLM in Ti:sapphire and Cr:forsterite lasers. Samples annealed at 700 °C had a faster relaxation time than those annealed at 550–600 °C, although the magnitude of the signal and therefore the saturation fluence was nearly the same as that of the sample annealed at 550 °C. Overall, higher annealing temperatures seem to be effective in improving the surface quality of the nanocrystallites and thereby reducing the saturation fluence, as previously demonstrated.[20]

The glass matrix surrounding the nanocrystallites is expected to strongly affect their surface properties and ultrafast dynamics. We fabricated films with InAs nanocrystallites doped into a borosilicate glass matrix (Ohara Optics, S-FSL5) and deposited them upon sapphire substrates to test the dependence of the absorption saturation dynamics on the glass matrix composition. The films were 10% InAs and 90% borosilicate glass; the composition of the glass was approximately 55–65% SiO_2, 15–25% K_2O, and 10–20% B_2O_3. Pump–probe measurements of these films demonstrated that, unlike in the SiO_2-based films, the pump–probe signal did not change discretely with annealing temperature, instead increasing continuously as the RTA temperature increased (Fig. 7). However, at high annealing temperatures the dynamics were similar to those measured with a SiO_2 matrix, and there was no significant improvement in the saturation fluence.

We believe that the difference in dependence on annealing temperature of films fabricated with InAs doped into a SiO_2 matrix and of films fabricated with InAs doped into a borosilicate glass matrix can be explained by examination of the different melting points of the composite films. The melting point of InAs is 942 °C, that of SiO_2 is 1710 °C, and that of borosilicate glass is ~727 °C. The eutectic point of each film is the temperature for a phase transition from solid to liquid for the composite film, which may be lower than the melting point of each film constituent.[25,26] Therefore, if the eutectic point for the composite InAs–glass film is within the range of the annealing temperature, the film will partially melt during RTA, and its properties will be different after it has cooled. Different eutectic points for the SiO_2-based films and the borosilicate glass–based films would cause the RTA to affect the film properties in dissimilar ways and could explain the dynamics observed in our experiments. For example, the difference in glass matrices would change the variation of nanocrystallite surface properties with RTA temperature for the SiO_2-based films compared with the borosilicate glass-based films, which could modify the saturation fluence. This variability demonstrates that the choice of glass and annealing temperature has an effect on the absorption saturation dynamics that must be considered when one is designing nonepitaxially grown semiconductor-doped silica films.

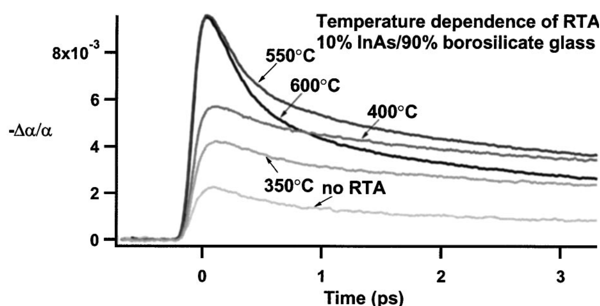

Fig. 7. Degenerate pump–probe measurement of a 10% InAs/90% borosilicate glass film at 800 nm. Measurements were made of films prepared with several rapid thermal annealing temperatures. The absorption saturation dynamics change continuously as a function of film annealing temperature.

5. GUIDELINES FOR OPTIMIZING SATURABLE ABSORBER PARAMETERS AND MODE-LOCKING RESULTS

We formulated guidelines from the experimental results described above to optimize the saturation fluence of semiconductor-doped silica film saturable absorbers for a given laser system. Linear transmission measurements (Fig. 1) showed that increasing the InAs/SiO_2 ratio shifts the onset of absorption to longer wavelengths, indicating an increased average nanocrystallite size in the films. By comparing the pump–probe measurements at 800 nm, 1.26 μm, and 1.5 μm taken of films with different InAs/SiO_2 ratios, one can see that films with larger nanocrystallites have significantly lower saturation fluence than those with smaller nanocrystallites, with a low saturation fluence of 640 $\mu J/cm^2$ measured for the 40% InAs/60% SiO_2 films at 1.54 μm. Furthermore, the tunable pump–probe measurements taken from 750 to 925 nm (Fig. 3) demonstrate that the saturation fluence decreases as the wavelength is tuned closer to the onset of absorption in the films. Finally, an annealing temperature higher than 550 °C resulted in strong absorption saturation, as shown in Figs. 6 and 7.

One can design semiconductor-doped silica films to produce low saturation fluence at a certain operating wavelength by observing the following guidelines. First, the semiconductor material and the semiconductor/glass ratio should be chosen to make the semiconductor nanocrystallites large while concurrently setting the onset of absorption near the laser wavelength. One can do this by choosing the bulk bandgap, E_g, of the semiconductor material to be slightly lower than the laser photon energy, E_p. When the semiconductor is incorporated into the glass film in the form of nanocrystallites and the semiconductor/glass ratio is appropriately selected, quantum-confinement effects will shift the absorption edge of the saturable-absorber film upward in energy toward E_p. The closer E_g is to E_p, the smaller the confinement-induced shift (as long as the shift is not greater than $E_p - E_g$). This keeps the nanocrystallites large while setting the onset of absorption in the film to be nearly at the operating wavelength and thus should minimize the saturation fluence. It is worth mentioning that, at high semiconductor/glass ratios, well-separated nanocrystallites may not be created, which could change the film properties.

The rapid thermal annealing temperature should be relatively high to optimize absorption saturation; however, the optimum temperature may vary for different semiconductor and glass materials and may need to be experimentally optimized. Finally, varying the RTA temperature can also tailor the carrier relaxation time for a particular application.

Figure 8 summarizes our investigations into characterizing the saturation fluence in our samples. A plot of the logarithm of the saturation fluence versus wavelength has been made based on the data described in Section 4 for films with different InAs/SiO_2 ratios (the 3% InAs/97% SiO_2 sample with the transmission curve shown in Fig. 1 was characterized at 800 nm in a separate measurement). From Fig. 8 it is clear that the saturation fluence decreases as the wavelength increases toward the onset of absorption. It should also be noted that the saturation fluence at 800 nm for the 3% InAs/97% SiO_2 film is higher than that of the 10% InAs/90% SiO_2 and 40% InAs/60% SiO_2 films, even though this wavelength is closer to its onset of absorption. We believe that this is so because of the small size of the nanocrystallites in this film and is another indicator of the general trend that saturation fluence decreases as nanocrystallite size decreases. Comparison of the various films at 800 nm illustrates how one can control the saturation fluence by varying the nanocrystallite size and the laser wavelength relative to the onset of absorption.

We applied the guidelines extracted from our experiments to design semiconductor-doped silica film saturable absorbers for self-starting KLM in a Cr:forsterite laser operating at 1.26 μm.[15] The linear and nonlinear optical properties of the 40% InAs/60% SiO_2 films described above were suitable for this application, as shown in Figs. 1 and 5(b). Films with a saturation fluence of 1.07 mJ/cm^2 at 1.26 μm were fabricated and used to self-start KLM in the 14-fs Cr:forsterite laser described above. Self-starting pulses were generated with 91-nm bandwidth and durations of 25 fs measured by interferometric autocorrelation. The mode-locking buildup time in this system was measured and found to be approximately 4.8 ms, approximately 10 times faster than that observed in Ti:sapphire[14]; this result can also be linked to the lower saturation fluence at this wavelength.

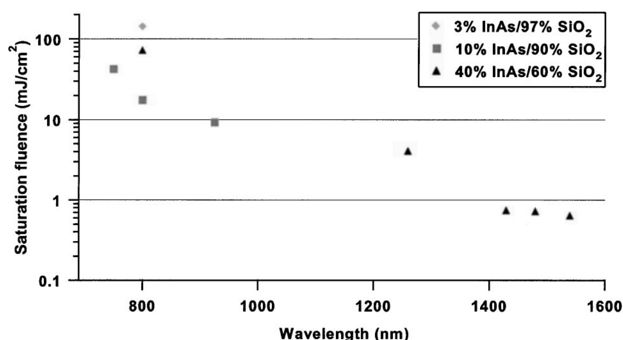

Fig. 8. Logarithmic plot of saturation fluence versus wavelength for 3% InAs/97% SiO_2, 10% InAs/90% SiO_2, and 40% InAs/60% SiO_2 films.

6. DISCUSSION AND CONCLUSIONS

The guidelines given above describe criteria for designing semiconductor-doped silica film devices with optimized saturation fluence. However, these materials still have relatively high saturation fluences compared with epitaxially grown devices and therefore have been used only to self-start KLM. One possible explanation for the high saturation fluences is based on the materials' rapid polarization dephasing time.[27] The dephasing time can be shown to be inversely proportional to the saturation fluence through equations that relate it to the homogeneous linewidth and absorption saturation cross section for a two-level system.[28] Fast polarization dephasing times of a few femtoseconds have been measured in semiconductor-doped glasses,[29] and the dephasing times in rf sputtered semiconductor-doped silica films are expected to be even faster because of the high density of defects in the sputtered films.

In previous research it was shown that the dephasing time in semiconductor nanocrystallites is dependent on the nanocrystallite size and surface quality, excitation wavelength relative to the band edge, and temperature.[30] The dephasing time increased with nanocrystallite size, operation closer to the absorption edge, better surface quality, and lower temperature. From our experimental results, a dependence of the saturation fluence on the nanocrystallite size, the annealing temperature (which should influence surface quality), and the excitation wavelength relative to the onset of absorption was observed. This correlation indicates that the fast polarization dephasing time in rf sputtered semiconductor-doped silica film saturable absorbers may be the primary limitation in achieving lower saturation fluences and better self-starting performance, although further experiments with films with smaller size distributions and well-controlled nanocrystallite properties will be necessary to verify this hypothesis. Other possible mechanisms that could contribute to the high saturation fluence in rf sputtered semiconductor-doped silica films include carrier–carrier or electron–phonon scattering and Auger recombination.[31]

In conclusion, guidelines for designing and fabricating nonepitaxially grown semiconductor-doped silica films with optimized saturation fluence for a given laser system were developed based on extensive characterization of the linear and nonlinear optical properties of these devices. A novel pump–probe system with independently tunable pump and probe wavelengths from 700 to 950 nm was developed for characterization of wavelength-dependent devices. The saturation fluence was found to be dependent on nanocrystallite size, wavelength of operation relative to the onset of absorption, and rapid thermal annealing temperature. Differences in the absorption saturation dynamics for different glass matrix materials were also observed. It was found that films annealed at high temperatures (above 550 °C for the samples tested) with large nanocrystallites and onset of absorption near the laser wavelength were optimal for laser mode-locking applications. Films with saturation fluences as low as 640 μJ/cm^2 at 1.54 μm were fabricated. Finally, a mechanism based on the fast dephasing time in semiconductor-

doped silica films was proposed to explain the high saturation fluence in these devices. Our plans for future research include applying nonepitaxially grown semiconductor saturable absorbers to other laser systems such as Cr:YAG, designing devices in different geometries, and exploring other methods for further reducing saturation fluence.

ACKNOWLEDGMENTS

We thank I. P. Bilinsky, C. Chudoba, M. S. Dresselhaus, F. X. Kaertner, J. Walpole, L. J. Misaggia, S. Saini, C. J. Stanton, and U. Morgner for their helpful assistance. This research is supported in part by U.S. Air Force Office of Scientific Research contract F49620-01-1-0084 and Medical Free Electron Laser Program contract F49620-01-1-0186 and by National Science Foundation contract ECS-0119452.

REFERENCES

1. D. E. Spence, P. N. Kean, and W. Sibbett, "60-fs pulse generation from a self-mode-locked Ti:sapphire laser," Opt. Lett. **16**, 42–44 (1991).
2. V. Magni, G. Cerullo, S. De Silvestri, and A. Monguzzi, "Astigmatism in Gaussian-beam self-focusing and in resonators for Kerr-lens mode locking," J. Opt. Soc. Am. B **12**, 476–485 (1995).
3. H. A. Haus and E. P. Ippen, "Self-starting of passively mode-locked lasers," Opt. Lett. **16**, 1331–1333 (1991).
4. U. Keller, D. A. B. Miller, G. D. Boyd, T. H. Chiu, J. F. Ferguson, and M. T. Asom, "Solid-state low-loss intracavity saturable absorber for Nd:YLF lasers: an antiresonant semiconductor Fabry–Perot saturable absorber," Opt. Lett. **17**, 505–507 (1992).
5. U. Keller, K. J. Weingarten, F. X. Kärtner, D. Kopf, B. Braun, I. D. Jung, R. Fluck, C. Hönninger, N. Matuschek, and J. Aus der Au, "Semiconductor saturable absorber mirrors (SESAMs) for femtosecond to nanosecond pulse generation in solid-state lasers," IEEE J. Sel. Top. Quantum Electron. **2**, 435–453 (1996).
6. S. Tsuda, W. H. Knox, S. T. Cundiff, W. Y. Jan, and J. E. Cunningham, "Mode-locking ultrafast solid-state lasers with saturable Bragg reflectors," IEEE J. Sel. Top. Quantum Electron. **2**, 454–464 (1996).
7. I. D. Jung, F. X. Kärtner, N. Matuschek, D. H. Sutter, F. Morier-Genoud, Z. Shi, V. Scheuer, M. Tilsch, T. Tschudi, and U. Keller, "Semiconductor saturable absorber mirrors supporting sub-10 fs pulses," Appl. Phys. B **65**, 137–150 (1997).
8. D. H. Sutter, G. Steinmeyer, L. Gallmann, N. Matuschek, F. Morier-Genoud, U. Keller, V. Scheuer, G. Angelow, and T. Tschudi, "Semiconductor saturable-absorber mirror assisted Kerr-lens mode-locked Ti:sapphire laser producing pulses in the two-cycle regime," Opt. Lett. **24**, 631–633 (1999).
9. R. Fluck, I. D. Jung, G. Zhang, F. X. Kärtner, and U. Keller, "Broadband saturable absorber for 10-fs pulse generation," Opt. Lett. **21**, 743–745 (1996).
10. S. Schön, M. Haiml, L. Gallmann, and U. Keller, "GaAs absorber layer growth for broadband AlGaAs/flouride SESAMs," J. Cryst. Growth **227**, 172–176 (2001).
11. N. Sarukura, Y. Ishida, T. Yanagawa, and H. Nakano, "All solid-state cw passively mode-locked Ti:sapphire laser using a colored glass filter," Appl. Phys. Lett. **57**, 229–230 (1990).
12. P. T. Guerreiro, S. Ten, N. F. Borrelli, J. Butty, G. E. Jabbour, and N. Peyghambarian, "PbS quantum-dot doped glasses as saturable absorbers for mode locking of a Cr:forsterite laser," Appl. Phys. Lett. **71**, 1595–1597 (1997).
13. I. P. Bilinsky, R. P. Prasankumar, and J. G. Fujimoto, "Self-starting mode locking and Kerr-lens mode locking of a Ti:Al_2O_3 laser by use of semiconductor-doped glass structures," J. Opt. Soc. Am. B **16**, 546–549 (1999).
14. I. P. Bilinsky, J. G. Fujimoto, J. N. Walpole, and L. J. Missaggia, "Semiconductor-doped silica saturable absorber films for solid-state laser mode locking," Opt. Lett. **23**, 1766–1768 (1998).
15. R. P. Prasankumar, C. Chudoba, J. G. Fujimoto, P. Mak, and M. F. Ruane, "Self-starting mode locking in a Cr:forsterite laser by use of non-epitaxially-grown semiconductor-doped silica films," Opt. Lett. **27**, 1564–66 (2002).
16. K. Tsunetomo, H. Nasu, H. Kitayama, A. Kawabuchi, Y. Osaka, and K. Takiyama, "Quantum size effect of semiconductor microcrystallites doped in SiO_2-glass thin films prepared by RF-sputtering," Jpn. J. Appl. Phys. **28**, 1928–1933 (1989).
17. K. Tsunetomo, M. Yamamoto, and Y. Osaka, "Preparation and properties of $In_xGa_{1-x}As$ microcrystallites embedded in SiO_2 glass films," Jpn. J. Appl. Phys. **30**, L521–L524 (1991).
18. S. Kaneko, H. Nasu, T. Ikegami, J. Matsuoka, and K. Kamiya, "Effect of preparation conditions on the properties of CdSe microcrystal-doped SiO_2 glass thin films prepared by RF-sputtering," Jpn. J. Appl. Phys. **31**, 2206–2211 (1992).
19. I. Tanahashi, A. Tsujimura, T. Mitsuyu, and A. Nishino, "Optical properties of CdS microcrystallite-doped SiO_2 glass thin films," Jpn. J. Appl. Phys. **29**, 2111–2115 (1990).
20. I. P. Bilinsky, J. G. Fujimoto, J. N. Walpole, and L. J. Missaggia, "InAs-doped silica films for saturable absorber applications," Appl. Phys. Lett. **74**, 2411–2413 (1999).
21. C. Hönninger, R. Paschotta, F. Morier-Genoud, M. Moser, and U. Keller, "*Q*-switching stability limits of continuous-wave passive mode locking," J. Opt. Soc. Am. B **46**, 46–56 (1999).
22. U. Morgner, F. X. Kärtner, S. H. Cho, Y. Chen, H. A. Haus, J. G. Fujimoto, E. P. Ippen, V. Scheuer, G. Angelow, and T. Tschudi, "Sub-two cycle pulses from a Kerr-lens mode-locked Ti:sapphire laser," Opt. Lett. **24**, 411–413 (1999).
23. R. L. Fork, O. E. Martinez, and J. P. Gordon, "Negative dispersion using pairs of prisms," Opt. Lett. **9**, 150–152 (1984).
24. C. Chudoba, J. G. Fujimoto, E. P. Ippen, H. A. Haus, U. Morgner, F. X. Kärtner, V. Scheuer, G. Angelow, and T. Tschudi, "All-solid-state Cr:forsterite laser generating 14-fs pulses at 1.3 μm," Opt. Lett. **26**, 292–294 (2001).
25. W. D. Callister, *Materials Science and Engineering: An Introduction* (Wiley, New York, 2003).
26. L. H. Van Vlack, *Elements of Materials Science* (Addison-Wesley, Reading, Mass., 1964).
27. I. P. Bilinsky, "Novel saturable absorber materials and devices for laser modelocking," Ph.D. dissertation (Massachusetts Institute of Technology, Cambridge, Mass., 1999).
28. A. E. Siegman, *Lasers* (University Science, Mill Valley, Calif., 1986).
29. G. L. Huang and H. S. Kwok, "Femtosecond dephasing times in semiconductor microcrystals measured with incoherent light," J. Opt. Soc. Am. B **9**, 2019–2024 (1992).
30. D. M. Mittleman, R. W. Schoenlein, J. J. Shiang, V. L. Colvin, A. P. Alivisatos, and C. V. Shank, "Quantum size dependence of femtosecond electronic dephasing and vibrational dynamics in CdSe nanocrystals," Phys. Rev. B **49**, 14,435–14,447 (1994).
31. V. I. Klimov, D. W. McBranch, C. A. Leatherdale, and M. G. Bawendi, "Electron and hole relaxation pathways in semiconductor quantum dots," Phys. Rev. B **60**, 13,740–13,749 (1999).